

# A Double-Functionalized Cyclen with Carbamoyl and Dansyl Groups (Cyclen = 1,4,7,10-Tetraazacyclododecane): A Selective Fluorescent Probe for $Y^{3+}$ and $La^{3+}$

Shin Aoki,<sup>†</sup> Hiroki Kawatani,<sup>†</sup> Teruhiro Goto,<sup>†</sup> Eiichi Kimura,<sup>\*,†</sup> and Motoo Shiro<sup>‡</sup>

Contribution from the Department of Medicinal Chemistry, Faculty of Medicine, Hiroshima University, Kasumi 1-2-3, Minami-ku, Hiroshima, 734-8551, Japan, and Rigaku Corporation X-ray Research Laboratory, Matsubaracho 3-9-12, Akishima, Tokyo, 196-8666, Japan

Received September 14, 2000

**Abstract:** A cyclen (=1,4,7,10-tetraazacyclododecane) doubly functionalized with three carbamoylmethyl groups and one dansylaminoethyl (dansyl = 2-(5-(dimethylamino)-1-naphthalenesulfonyl) group ( $L^2 = 1$ -(2-(5-(dimethylamino)-1-naphthalenesulfonylamido)ethyl)-4,7,10-tris(carbamoylmethyl)-cyclen) was synthesized and characterized. Potentiometric pH titration and UV spectrophotometric titration of  $L^2$  served to determine deprotonation of the pendant dansylamide ( $L^2 \rightarrow H_{-1}L^2$ ) with a  $pK_a$  value of 10.6, while the fluorometric titration disclosed a  $pK_a$  value of  $8.8 \pm 0.2$ , which was assigned to the dansyl deprotonation in the excited state. The 1:1  $M^{3+}-H_{-1}L^2$  complexation constants ( $\log K_{app} = 6.0$  for  $Y^{3+}$  and 5.2 for  $La^{3+}$ , where  $K_{app}(M-H_{-1}L^2) = [M^{3+}-H_{-1}L^2]/[M^{3+}]_{free}[L^2]_{free}$  ( $M^{-1}$ ) at pH 7.4) were determined by potentiometric pH titration and UV and fluorescence spectrophotometric titrations (excitation at 335 nm and emission at 520 nm) in aqueous solution (with  $I = 0.1$  (NaNO<sub>3</sub>)) and 25 °C. The X-ray structure analysis of the  $Y^{3+}-H_{-1}L$  complex showed nine-coordinated  $Y^{3+}$  with four nitrogens of cyclen, three carbamoyl oxygens, and the deprotonated nitrogen and a sulfonyl oxygen of the dansylamide. The crystal data are as follow: formula  $C_{28}H_{49}N_{11}O_{13.5}SY$  ( $Y^{3+}-H_{-1}L^2 \cdot 2(NO_3^-) \cdot 2.5H_2O$ ),  $M_r = 876.73$ , monoclinic, space group  $P2_1/n$  (No. 14),  $a = 18.912(3)$  Å,  $b = 17.042(3)$  Å,  $c = 24.318(4)$  Å,  $\beta = 95.99(1)^\circ$ ,  $V = 7794(2)$  Å<sup>3</sup>,  $Z = 8$ ,  $R1 = 0.099$ . Upon  $M^{3+}-H_{-1}L^2$  complexation, the dansyl fluorescence greatly increased (8.6 and 3.8 times for  $Y^{3+}$  and  $La^{3+}$ , respectively) in aqueous solution at pH 7.4. Other lanthanide ions also yielded  $Ln^{3+}-H_{-1}L^2$  complexes with similar  $K_{app}$  values, although all the dansyl fluorescences were weakly quenched. On the other hand, zinc(II) formed only a 1:1  $Zn^{2+}-L^2$  complex at neutral pH with negligible fluorescence change. The X-ray crystal structure of the  $Zn^{2+}-L^2$  complex confirmed the pendant dansylamide being noncoordinating. The crystal data are as follow: formula  $C_{28}H_{51}N_{11}O_{14}SZn$  ( $Zn^{2+}-L^2 \cdot 2(NO_3^-) \cdot 3H_2O$ ),  $M_r = 863.22$ , monoclinic, space group  $C2/n$  (No. 15),  $a = 35.361(1)$  Å,  $b = 13.7298(5)$  Å,  $c = 18.5998(6)$  Å,  $\beta = 119.073(2)^\circ$ ,  $V = 7892.3(5)$  Å<sup>3</sup>,  $Z = 8$ ,  $R1 = 0.084$ . Other divalent metal ions did not interact with  $L^2$  at all (e.g.,  $Mg^{2+}$  and  $Ca^{2+}$ ) or interacted with  $L^2$  with the dansyl fluorescence quenched (e.g.,  $Cu^{2+}$ ).

## Introduction

Macrocyclic polyamines including cyclen (=1,4,7,10-tetraazacyclododecane) with attached acetates or carbamoylmethyls are useful ligands for lanthanide(III) ions in aqueous solution.<sup>1–3</sup> The resulting 1:1 complexes are kinetically and thermodynamically stable and useful for magnetic resonance imaging (e.g., Gd),<sup>1c</sup> radiotherapeutic applications (e.g., Y),<sup>4</sup> or catalysis (e.g., Y, La, and Yb).<sup>5</sup> Morrow found that among cationic  $Ln^{3+}$  ( $Ln = La, Eu, Dy$ ) tetrakis(carbamoylmethyl)cyclen complexes,

$[Ln-(TCMC)]^{3+}$  (e.g., **1** where  $Ln = La$ ) efficiently promoted RNA cleavage<sup>6</sup> (TCMC = 1,4,7,10-tetrakis(carbamoylmethyl)-cyclen, which is also called DOTAM<sup>2,7</sup>). Characterization including an X-ray crystal structure of  $[Ln-(TCMC)]^{3+}$  indicated strong coordination of the carbamoyl groups.<sup>6a,c</sup> The

\* To whom correspondence should be addressed. E-mail: ekimura@hiroshima-u.ac.jp.

<sup>†</sup> Hiroshima University.

<sup>‡</sup> Rigaku Corp.

(1) (a) Alexander, V. *J. Chem. Rev.* **1995**, *95*, 273–342. (b) Parker, D.; Williams, J. A. G. *J. Chem. Soc., Dalton Trans.* **1996**, 3613–3628. (c) Caravan, P.; Ellison, J. J.; McMurry, T. J.; Lauffer, R. B. *Chem. Rev.* **1999**, *99*, 2293–2352.

(2) (a) Martell, A. E.; Hancock, R. D. *Metal Complexes in Aqueous Solutions*; Plenum Press: New York, 1996. (b) Hancock, R. D.; Martell, A. E. *Chem. Rev.* **1989**, *89*, 1875–1914.

(3) de Silva, A. P.; Gunaratne, H. Q. N.; Gunnlaugsson, T.; Huxley, A. J. M.; McCoy, C. P.; Rademacher, J. T.; Rice, T. E. *Chem. Rev.* **1997**, *97*, 1515–1566.

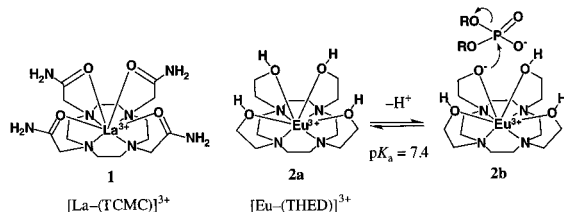
(4) (a) Anderson, C. J.; Welch, M. J. *Chem. Rev.* **1999**, *99*, 2219–2234. (b) Volkert, W. A.; Hoffman, T. J. *Chem. Rev.* **1999**, *99*, 2269–2292. (c) Takeunouchi, K.; Watanabe, K.; Kato, Y.; Koike, T.; Kimura, E. *J. Org. Chem.* **1993**, *58*, 1955–1958. (d) Takenouchi, K.; Tabe, M.; Watanabe, K.; Hazato, A.; Kato, Y.; Shionoya, M.; Koike, T.; Kimura, E. *J. Org. Chem.* **1993**, *58*, 6895–6899. (e) Moi, M. K.; DeNardo, S. J.; Meares, C. F. *Cancer Res.* **1990**, *50* (Suppl.), 789s–793s.

(5) (a) Shibusaki, M.; Sasai, H.; Arai, T. *Angew. Chem., Int. Ed. Engl.* **1997**, *36*, 1237–1256. (b) Kobayashi, S. In *Organic Synthesis in Water*; Grieco, P. A. Ed.; Blackie Academic & Professional: London, 1998; pp 262–305.

(6) (a) Amin, S.; Morrow, J. R.; Lake, C. H.; Churchill, M. R. *Angew. Chem., Int. Ed. Engl.* **1994**, *33*, 773–775. (b) Morrow, J. R.; Amin, S.; Lake, C. H.; Churchill, M. R. *Inorg. Chem.* **1993**, *32*, 4566–4572. (c) Amin, S.; Voss, D. A.; Horrocks, W. D., Jr.; Lake, C. H.; Churchill, M. R.; Morrow, J. R. *Inorg. Chem.* **1994**, *33*, 3294–3300.

(7) (a) Carlton, L.; Hancock, R. D.; Maumela, H.; Wainwright, K. P. J. *J. Chem. Soc., Chem. Commun.* **1994**, 1007–1008. (b) Maumela, H.; Hancock, R. D.; Carlton, L.; Reibenspies, J. H.; Wainwright, K. P. *J. Am. Chem. Soc.* **1995**, *117*, 6698–6707.

dramatic difference in the reactivity of  $[\text{Ln}-(\text{TCMC})]^{3+}$  in RNA cleavage was attributed to the larger number of coordination sites of the larger  $\text{La}^{3+}$  complexes compared to other  $\text{Ln}^{3+}$  complexes, whereby RNA phosphodiester interacted with  $\text{La}^{3+}$ .



On the other hand, among  $\text{Ln}^{3+}$  complexes with tetrakis-(hydroxyethylcyclen) (THED),  $[\text{Eu}-(\text{THED})]^{3+}$  **2** was the most efficient catalyst in the hydrolysis of phosphate diesters, due to the higher acidity of the  $\text{Eu}^{3+}$  complex. One of the metal-bound hydroxyls deprotonated to **2b** with a  $pK_a$  of 7.4, which provided a strong nucleophile to attack phosphate esters.<sup>8</sup> It is apparent that  $\text{Ln}^{3+}$  remained as strong Lewis acids in these chelates, as illustrated by the  $pK_a$  value of 7.4 for a pendant alcohol in **2**.

Zinc(II) ions, biologically the most useful Lewis acid, have been extensively explored as catalysts for ester hydrolyses.<sup>9,10</sup> For instance, a hydroxyethylcyclen<sup>10a,b</sup> efficiently cleaves phosphodiester such as the  $\text{Eu}^{3+}$  complex **2b** at neutral pH. Recently, the acidic properties of  $\text{Zn}^{2+}$  were used with a dansyl-pendant cyclen **3a** ( $L^1$ ),<sup>11</sup> whereby a nanomolar concentration of  $\text{Zn}^{2+}$  was sensed in the deprotonated amide binding complex **3b** ( $\text{Zn}^{2+}-\text{H}_-L^1$ ) with strong fluorescent emission.<sup>12</sup>

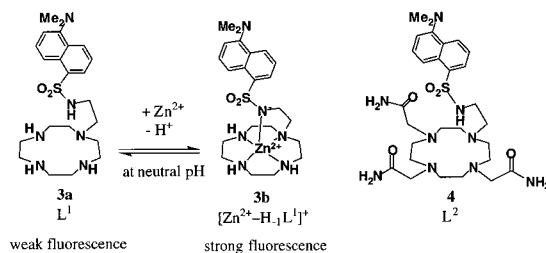
(8) For other examples of  $\text{Ln}^{3+}$ -promoted RNA cleavage, see: Magda, D.; Miller, R. A.; Sessler, J. L.; Iverson, B. L. *J. Am. Chem. Soc.* **1994**, *116*, 7439–7440 and references therein.

(9) For other reviews, see: (a) Kimura, E.; Shionoya, M. In *Transition Metals in Supramolecular Chemistry*; Fabbrizzi, L., Poggi, A., Eds.; Kluwer Academic Publishers: Dordrecht, 1994; pp 245–259. (b) Kimura, E. In *Progress in Inorganic Chemistry*; Karlin, K. D., Ed.; John Wiley & Sons: New York, 1994; Vol. 41, pp 443–491. (c) Kimura, E.; Shionoya, M. In *Metal Ions in Biological Systems*; Sigel, A., Sigel, H., Eds.; Marcel Dekker: New York, 1996; Vol. 33, pp 29–52. (d) Kimura, E.; Koike, T.; Aoki, S. *J. Synth. Org. Chem., Jpn.* **1997**, *55*, 1052–1061. (e) Kimura, E.; Koike, T. *J. Chem. Soc., Chem. Commun.* **1998**, 1495–1500. (f) Kimura, E.; Koike, T. In *Bioinorganic Catalysis*; Reedijk, J., Bouwman, E., Eds.; Marcel Dekker: New York, 1999; pp 33–54. (g) Kimura, E. *Curr. Opin. Chem. Biol.* **2000**, *4*, 207–213. (h) Kimura, E.; Kikuta, E. *J. Biol. Inorg. Chem.* **2000**, *5*, 139–155.

(10) (a) Koike, T.; Kajitani, S.; Nakamura, I.; Kimura, E.; Shiro, M. *J. Am. Chem. Soc.* **1995**, *117*, 1210–1219. (b) Kimura, E.; Kodama, Y.; Koike, T.; Shiro, M. *J. Am. Chem. Soc.* **1995**, *117*, 8304–8311. (c) Kimura, E.; Hashimoto, H.; Koike, T. *J. Am. Chem. Soc.* **1996**, *118*, 10963–10970. (d) Koike, T.; Inoue, M.; Kimura, E.; Shiro, M. *J. Am. Chem. Soc.* **1996**, *118*, 3091–3099.

(11) (a) Koike, T.; Watanabe, T.; Aoki, S.; Kimura, E.; Shiro, M. *J. Am. Chem. Soc.* **1996**, *118*, 12696–12703. (b) Koike, T.; Kimura, E.; Nakamura, I.; Hashimoto, Y.; Shiro, M. *J. Am. Chem. Soc.* **1992**, *114*, 7338–7345. For reviews, see: (c) Kimura, E. *S.-Afr. Tydskr. Chem.* **1997**, *50*, 240–248. (d) Kimura, E.; Koike, T. *Chem. Soc. Rev.* **1998**, *27*, 179–184. The ligand **4**·5HCl is commercially available from Dojindo Laboratories, Japan.

(12) For other zinc(II) fluorophores, see: (a) Czarnik, A. W. *Acc. Chem. Res.* **1994**, *27*, 302–308. (b) Zalewski, P. D.; Forbes, I. J.; Seamark, R. F.; Borlinghaus, R.; Betts, W. H.; Lincoln, S. F.; Ward, A. D. *Chem. Biol.* **1994**, *1*, 153–161. (c) Hendrickson, K. M.; Rodopoulos, T.; Pittet, P.-A.; Mahadevan, I.; Lincoln, S. F.; Ward, A. D.; Kurucsev, T.; Duckworth, P. A.; Forbes, I. J.; Zalewski, P. D.; Betts, W. H. *J. Chem. Soc., Dalton Trans.* **1997**, 3879–3882. (d) Godwin, H. A.; Berg, J. M. *J. Am. Chem. Soc.* **1996**, *118*, 6514–6515. (e) Walkup, G. K.; Imperiali, B. *J. Am. Chem. Soc.* **1997**, *119*, 3443–3450. (f) Thompson, R. B.; Maliwal, B. P.; Fierke, C. A. *Anal. Chem.* **1998**, *70*, 1749–1754. (g) Sarwar Nasir, M.; Fahrni, C. J.; Suhy, D. A.; Kolodisick, K. J.; Singer, C. P.; O'Halloran, T. V. *J. Biol. Inorg. Chem.* **1999**, *4*, 775–783. (h) Reany, O.; Gunnlaugsson, T.; Parker, D. *J. Chem. Soc., Chem. Commun.* **2000**, 473–474. (i) Hirano, T.; Kikuchi, K.; Urano, Y.; Higuchi, T.; Nagano, T. *Angew. Chem., Int. Ed. Engl.* **2000**, *39*, 1052–1054. (j) Walkup, G. K.; Burdette, S. C.; Lippard, S. J.; Tsien, R. Y. *J. Am. Chem. Soc.* **2000**, *122*, 5644–5645.

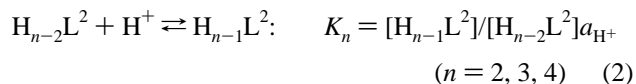
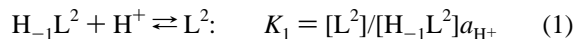


In an effort to design useful fluorescent sensors for  $\text{La}^{3+}$  and other relevant  $\text{M}^{3+}$ , by using the principle of  $\text{Zn}^{2+}$ –**3a** complexation, we now have incorporated three carbamoylmethyl pendants to **3a** to make **4** ( $L^2$ ). The three carbamoylmethyl pendant might affect the microenvironment surrounding the fluorescent dansyl pendant. After this work was almost finished, Lowe and Parker independently reported the pH-dependent luminescence properties of  $\text{Eu}^{3+}$ - and  $\text{Tb}^{3+}$ -cyclens appended with an aryl-sulfonamide and three acetate groups.<sup>13</sup> This paper describes metal-dependent ligation of the sulfonamide and the resulting dansyl fluorescence responses. It is of interest that **4** allowed a direct comparison of characteristic acid and coordinating properties of lanthanide(III) ions and zinc(II) ion.<sup>14</sup>

## Results

**Synthesis of 1-Dansylamidoethyl-4,7,10-tris(carbamoylmethyl)-cyclen  $L^2$  (**4**).** The ligand **4** was synthesized as shown in Scheme 1. The mono-*N*-Cbz-cyclen **7** was obtained as the 3HCl salt by reaction of 3Boc-cyclen **5**<sup>15</sup> with benzyl chloroformate (CbzCl) and successive deprotection of three Boc groups of **6**. The acid-free **7** was alkylated with 2-bromoacetoamide to give **8**, whose Cbz group was removed by a conventional method ( $\text{H}_2$ , Pd/C) to afford **9**. Successive alkylation of **9** with **10** gave **4**, which was isolated as the 3HCl salt.

**Determination of Protonation Constants for  $L^2$ .** The protonation constants ( $K_n$ ) of **4** ( $L^2$ ) were determined by potentiometric and spectrophotometric pH titrations of  $4 \cdot 3\text{HCl} \cdot 2\text{H}_2\text{O}$  (1 mM) against 0.10 mM NaOH with  $I = 0.10$  ( $\text{NaNO}_3$ ) at 25 °C. A typical potentiometric pH titration curve is shown in Figure 1a, which indicates dissociation of four protons at  $0 < \text{eq}(\text{OH}^-) < 4$ . The titration data were analyzed for the acid–base equilibria 1 and 2, where  $a_{\text{H}^+}$  is the activity of  $\text{H}^+$ . The four protonation constants,  $K_1$ ,  $K_2$ ,  $K_3$ , and  $K_4$ , were calculated by using the program BEST,<sup>16</sup> as summarized in logarithmic numbers in Scheme 2.



(13) Lowe, M. P.; Parker, D. *J. Chem. Soc., Chem. Commun.* **2000**, 707–708.

(14) For previous examples of luminiscent lanthanide(III) complexes, see: (a) Alpha, B.; Lehn, J.-M.; Mathis, G. *Angew. Chem., Int. Ed. Engl.* **1987**, *26*, 266–267. (b) Alpha, B.; Balzani, V.; Lehn, J.-M.; Perathoner, S.; Sabbatini, N. *Angew. Chem., Int. Ed. Engl.* **1987**, *26*, 1266–1267. (c) Balzani, V.; Lehn, J.-M.; van de Loosdrecht, J.; Mecati, A.; Sabbatini, N.; Ziessel, R. *Angew. Chem., Int. Ed. Engl.* **1991**, *30*, 190–191. (d) Saha, A. K.; Kross, K.; Kloszewski, E. D.; Upson, D. A.; Toner, J. L.; Anow, R. A.; Black, C. D. V.; Desai, V. C. *J. Am. Chem. Soc.* **1995**, *115*, 11032–11033. (e) Gunnlaugsson, T.; Parker, D. *J. Chem. Soc., Chem. Commun.* **1998**, 511–512.

(15) Kimura, E.; Aoki, S.; Koike, T.; Shiro, M. *J. Am. Chem. Soc.* **1997**, *119*, 3068–3076.

(16) Martell, A. E.; Motekaitis, R. J. *Determination and Use of Stability Constants*, 2nd ed.; VCH: New York, 1992.

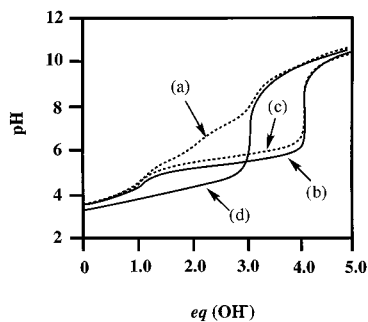
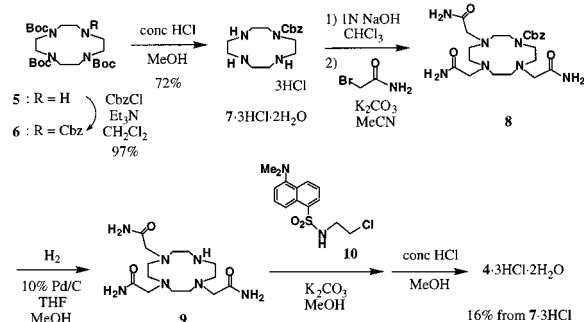
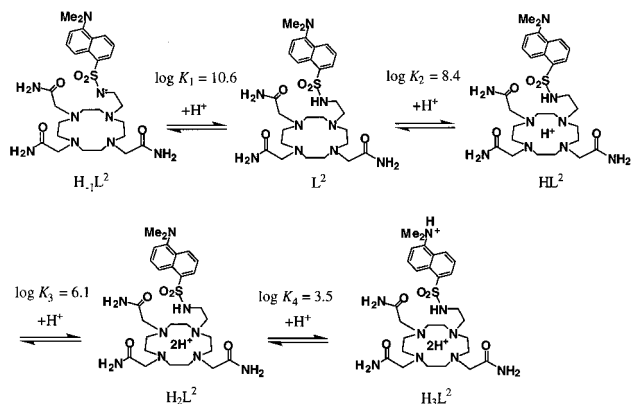


**Figure 1.** Typical pH titration curves of 1 mM **4** (a), 1 mM **4** + 1 mM  $Y^{3+}$  (b), 1 mM **4** + 1 mM  $La^{3+}$  (c), and 1 mM **4** + 1 mM  $Zn^{2+}$  (d) at 25 °C with  $I = 0.1$  ( $NaNO_3$ ), where  $eq(OH^-)$  is the number of equivalents of base added.

### Scheme 1



### Scheme 2



The assignment of the four protonation mode shown in Scheme 2 is based on the following facts: (i) diprotonated TCMC (=DOTAM)<sup>2</sup> had two protonation constants of 7.5 and 6.0 (Table 1);<sup>7b,17</sup> (ii) the pH-dependent UV spectral change for **4** at 25 °C with  $I = 0.1$  ( $NaNO_3$ ) (see below) gave a  $pK_1$  value of 10.6, assignable to  $ArSO_2N^-R (H_{-1}L^2) + H^+ \rightleftharpoons ArSO_2NHR (L^2)$ ; and (iii) the  $\log K_4$  value of 3.5 was assigned for  $ArN(Me)_2 (H_2L^2) + H^+ \rightleftharpoons ArN^+H(Me)_2 (H_3L^2)$  by analogy with the  $\log K_4$  value of 4.0 for **3a**<sup>11a</sup> (and by the UV absorption spectral change of **4** at pH 2–6).

**The UV and Fluorescence Spectral Titration of 4 ( $L^2$ ).** We examined the pH-dependent UV and fluorescence properties of **4**. As shown in Figure 2a, **4** has an absorption maximum at 330 nm ( $\epsilon = 4.5 \times 10^3 \text{ M}^{-1}\cdot\text{cm}^{-1}$ ) at pH 7.4 (50 mM HEPES with  $I = 0.1$  ( $NaNO_3$ ) and 25 °C (**3a** has an absorption maximum at 330 nm with  $\epsilon = 4.95 \times 10^3 \text{ M}^{-1}\cdot\text{cm}^{-1}$  at pH 7.3 with  $I = 0.10$  ( $NaNO_3$ )<sup>11a</sup>). Deprotonation of the sulfonamide NH of dansyl pendant ( $ArSO_2N^-R (H_{-1}L^2) + H^+ \rightleftharpoons ArSO_2-$

**Table 1.** Protonation Constants [ $\log K_n$  and  $\log K_5(M-H_{-1}L)$ ] and Complexation Constants [ $\log K(M-L)$ ,  $\log K_{app}(M-H_{-1}L)$  at pH 7.4] of Cyclen, TCMC, **3a**, and **4** at 25 °C with  $I = 0.1$  ( $NaNO_3$ )<sup>a</sup>

	cyclen <sup>b</sup>	TCMC	<b>3a</b> <sup>e</sup>	<b>4</b>
$\log K_1$	11.0	7.5 <sup>c</sup> (7.7) <sup>d</sup>	11.8	10.6
$\log K_2$	9.9	6.0 <sup>c</sup> (6.2) <sup>d</sup>	10.8	8.4
$\log K_3$	<2	<2 <sup>c</sup>	9.4	6.1
$\log K_4$	<2	<2 <sup>c</sup>	4.0	3.5
$\log K(Zn-L)$	15.3	10.5 <sup>d</sup>	20.8	11.8
$\log K_5(Zn-H_{-1}L)$			5.0	10.7
$\log K(Y-L)$			6.0	
$\log K_5(Y-H_{-1}L)$			5.5	
$\log K_{app}(Y-H_{-1}L)$			neg <sup>f</sup>	6.0 <sup>g</sup>
$\log K(La-L)$		10.4 <sup>d</sup>		5.5
$\log K_5(La-H_{-1}L)$			6.2	
$\log K_{app}(La-H_{-1}L)$			neg <sup>f</sup>	5.2 <sup>g</sup>

<sup>a</sup> For the definitions of  $K_n$ ,  $K(M-L)$ ,  $K_5(M-H_{-1}L)$ , and  $K_{app}(M-H_{-1}L)$ , see the text. The same titration was carried out at least twice, and the experimental errors were  $\pm 3\%$ . <sup>b</sup> From ref 10a at 25 °C with  $I = 0.1$  ( $NaNO_3$ ). <sup>c</sup> Reference 17. <sup>d</sup> From ref 7b at 25 °C in 0.1 M  $NaNO_3$ . <sup>e</sup> From ref 11a at 25 °C with  $I = 0.1$  ( $NaNO_3$ ). <sup>f</sup> neg = negligible. The addition of  $Y^{3+}$  or  $La^{3+}$  to **3a** had negligible effects on UV absorption and fluorescence emission spectra. <sup>g</sup> At pH 7.4.

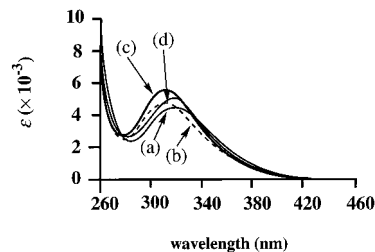


**Figure 2.** UV-pH profile for **4** (0.1 mM) at 25 °C with  $I = 0.1$  ( $NaNO_3$ ), (a) at pH 7.4,  $\lambda_{max} = 330 \text{ nm}$  ( $\epsilon = 4.5 \times 10^3$ ); (b) at pH 11.8,  $\lambda_{max} = 320 \text{ nm}$  ( $\epsilon = 4.7 \times 10^3$ ); (c) +2 equiv of  $Y^{3+}$  at pH 7.4; (d) +2 equiv of  $La^{3+}$  at pH 7.4.

NHR ( $L^2$ )) caused the UV absorption spectral change from curve (a) at pH 7.4 to curve (b) at pH 11.8, from which the  $pK_1$  value of 10.6 was determined. Figure 3a compares pH-dependent changes in the  $\epsilon$  value at 320 nm for **3a** and **4** with  $I = 0.1$  ( $NaNO_3$ ) at 25 °C.

Curve (a) in Figure 4 shows a fluorescence emission spectrum of 10  $\mu\text{M}$  **4** ( $\Phi$  (quantum yield) = 0.03) at pH 7.4 (10 mM HEPES with  $I = 0.1$  ( $NaNO_3$ )), which is almost the same curve as that of **3a** under the same conditions. A remarkable difference between **3a** and **4** was seen in the pH-dependent fluorescence titration of the dansyl in 10 mM Good's buffer solutions (Figure 3b). While the fluorescence emission intensity ( $I$ ) of **3a** at 520 nm (excitation at 335 nm) increased by only ca. 30% with a  $pK_a$  of 11.8, that of **4** increased dramatically ( $I/I_0 = 8.5$ , where  $I_0$  is the fluorescence intensity of **4** (10  $\mu\text{M}$ ) at pH 7.4 and 25 °C) (see curve (b) in Figure 4) with a much smaller  $pK_a$  of  $8.8 \pm 0.2$ . A quantum yield of **4** at pH 11.0 ( $\Phi = 0.18$ ) is 6 times larger than that at pH 7.4 (0.03) (excitation at 335 nm) (this latter value is almost the same as that of **3a** at pH 7.4 (0.03)<sup>11a</sup>). The pH-dependent fluorescence curve for **4** (Figure 3b) fit to the sum of population of  $L^2$  and  $H_{-1}L^2$  in the speciation diagram of **4** (Figure 3c). It is concluded that the break at pH 8.8 in Figure 3b denotes the  $pK_a$  for  $(HL^2)^+ \rightleftharpoons L^2$ , and, at the same time, the strong fluorescence due to unprotonated  $L^2$  predominates in Figure 3b for **4**. It is suggested that, upon total removal of protons from the cyclen moiety, three carbamoyl groups may somehow work to create a hydrophobic microenvironment around the dansyl group to increase the fluorescence. Naphthyl fluorescent probes are well known to dramatically increase the

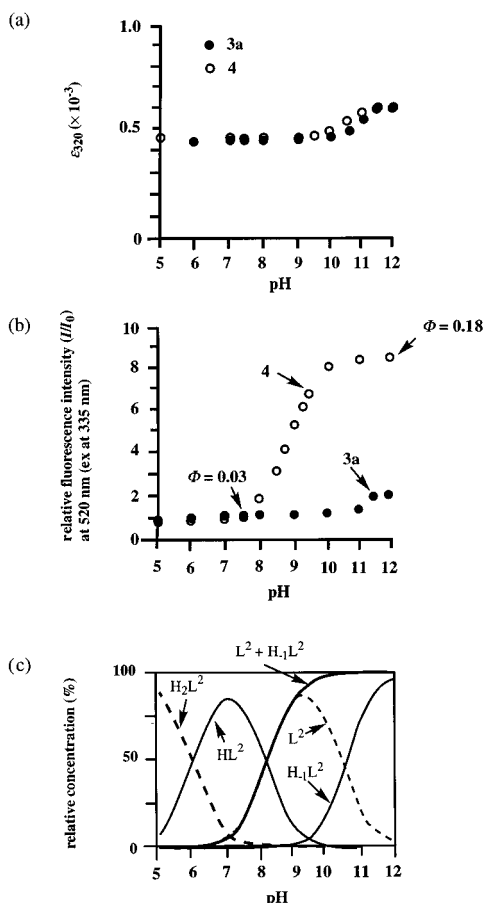


**Figure 3.** pH-dependent UV (a) and fluorescence (b) changes of **3a** (black circles) and **4** (white circles) at 25 °C. [**3a** or **4**] = 0.1 mM for UV titration and [**3a** or **4**] = 10 μM for fluorescence titration.  $I_0$  is the fluorescence intensity of **4** (10 μM) at 520 nm and pH 7.4. (c) Speciation diagram for 10 μM **4** at 25 °C with  $I = 0.1$  (NaNO<sub>3</sub>).

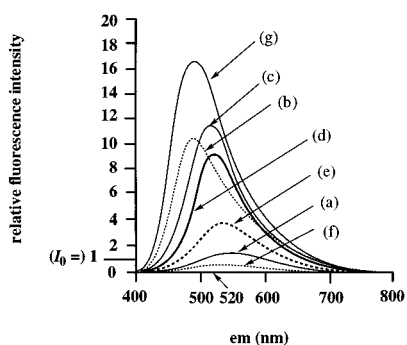


**Figure 4.** Fluorescence emission spectra of 10 μM **4** at 25 °C with  $I = 0.1$  (NaNO<sub>3</sub>). (a) at pH 7.4 ( $\Phi = 0.03$ ); (b) at pH 11.0 ( $\Phi = 0.18$ ); (c) in MeCN ( $\Phi = 0.19$ ); (d) +30 μM Y<sup>3+</sup> ( $\Phi = 0.13$ ); (e) +30 μM La<sup>3+</sup> ( $\Phi = 0.08$ ); (f) +30 μM Eu<sup>3+</sup> ( $\Phi = 0.01$ ); (g) Y<sup>3+</sup>–H<sub>−1</sub>L<sup>2</sup> complex (**12a**) in MeCN ( $\Phi = 0.26$ ).

fluorescence intensities in a hydrophobic environment.<sup>18,19</sup> Interestingly, the fluorescence of uncomplexed **4** (10 μM) in MeCN solution (curve (c) in Figure 4) was as strong as the

(18) (a) Li, Y.-H.; Chan, L.-M.; Tyer, L.; Moody, R. T.; Himel, C. M.; Hercules, D. M. *J. Am. Chem. Soc.* **1975**, *97*, 3118–3126. (b) Cardona, C. M.; Alvarez, J.; Kaifer, A. E.; McCarley, T. D.; Pandey, S.; Baker, G. A.; Bonzagni, N. J.; Bright, F. V. *J. Am. Chem. Soc.* **2000**, *122*, 6139–6144.

(19) (a) Ikeda, H.; Nakamura, M.; Ise, N.; Oguma, N.; Nakamura, A.; Ikeda, T.; Toda, F.; Ueno, A. *J. Am. Chem. Soc.* **1996**, *118*, 10980–10988. (b) Ueno, A.; Ikeka, A.; Ikeda, H.; Ikeda, T.; Toda, F. *J. Org. Chem.* **1999**, *64*, 382–387. (c) Bügler, J.; Engbersen, J. F. J.; Reinhoudt, D. N. *J. Org. Chem.* **1998**, *63*, 5339–5344. (d) Matsumura, S.; Sakamoto, S.; Ueno, A.; Mihara, H. *Chem. Eur. J.* **2000**, *6*, 1781–1788.

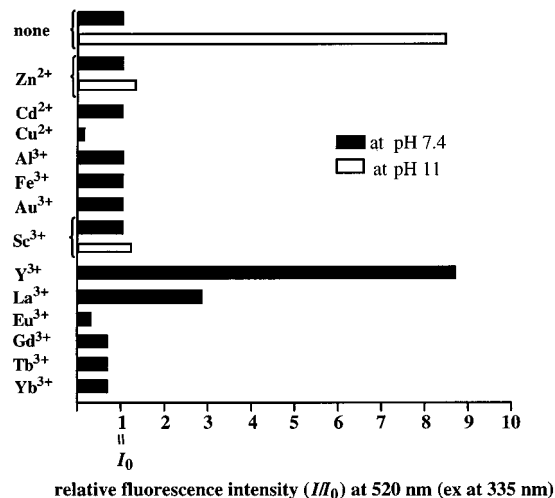


**Figure 5.** Relative fluorescence intensity of **4** (10 μM) responding to 2 equiv of metal ions at pH 7.4 (10 mM HEPES) and pH 11.0 (10 mM CAPS) and 25 °C with  $I = 0.1$  (NaNO<sub>3</sub>) based on the fluorescence intensity height at 520 nm (excitation at 335 nm) and pH 7.4.

fluorescence in pH 11.0 aqueous solution (curve (b) in Figure 4). Similarly strong emissions were observed with uncomplexed **3a** and *N*-dansyl-L-valine in MeCN/10 mM HEPES (pH 7.4 with  $I = 0.1$  (NaNO<sub>3</sub>)) (99/1).<sup>18</sup> However, **3a** in pH 11 aqueous solution gave a much weaker emission.

#### Characteristic Fluorescent Responses of **4** to Metal Ions.

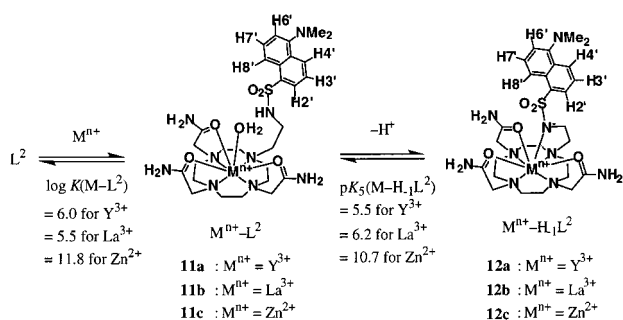
We tested the fluorescent responses of **4** (10 μM) to various metal ions at pH 7.4 (10 mM HEPES with  $I = 0.1$  (NaNO<sub>3</sub>)) and 25 °C (excitation at 335 nm, which is an isosbestic point determined by UV titrations).<sup>20</sup> As summarized in Figure 5, the fluorescence of **4** at 520 nm was not affected by 1–2 equiv of Zn<sup>2+</sup>, Cd<sup>2+</sup>, Al<sup>3+</sup>, Fe<sup>3+</sup>, Au<sup>3+</sup>, Sc<sup>3+</sup>, Li<sup>+</sup>, Na<sup>+</sup>, K<sup>+</sup>, Mg<sup>2+</sup>, Ca<sup>2+</sup>, or Fe<sup>2+</sup>. On the other hand, Y<sup>3+</sup> and La<sup>3+</sup> greatly enhanced the emission (8.6 and 3.8 times, respectively, with 2 equiv each). It is of particular interest that **4** did not sense Zn<sup>2+</sup>, although **4** would complex with Zn<sup>2+</sup>. The emission of **4** was more or less quenched by Cu<sup>2+</sup>, Eu<sup>3+</sup>, Gd<sup>3+</sup>, Tb<sup>3+</sup>, and Yb<sup>3+</sup>. These results imply that **4** could be a selective fluorescence probe for Y<sup>3+</sup> and La<sup>3+</sup> at neutral pH in aqueous solution (vide infra).

Figure 4 compares the fluorescence spectra of **4** at various conditions. Curves (d)–(f) are emission spectra of **4** in the presence of 3 equiv of Y<sup>3+</sup> ( $\Phi = 0.13$ ), La<sup>3+</sup> ( $\Phi = 0.08$ ), and Eu<sup>3+</sup> ( $\Phi = 0.01$ ), respectively. As described later, the Y<sup>3+</sup>–H<sub>−1</sub>L<sup>2</sup> complex **12a** was isolated, which afforded a much larger quantum yield of 0.26 in MeCN/10 mM HEPES (pH 7.4 with  $I = 0.1$  (NaNO<sub>3</sub>)) (99/1) or MeCN (curve (g) in Figure 4).

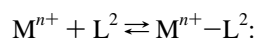
**Complexation of **4** with Zn<sup>2+</sup>, Y<sup>3+</sup>, and La<sup>3+</sup> by Potentiometric pH Titration.** Complexation of **4** with zinc(II), yttrium(III), and lanthanum(III) ions were studied by potentiometric pH titration of **4**·3HCl (1 mM) in the presence of an equimolar amount of the metal ions at 25 °C with  $I = 0.1$  (NaNO<sub>3</sub>) (see Figure 1b–d). The titration curves for Y<sup>3+</sup> (curve (b)) and La<sup>3+</sup> (curve (c)) revealed the formation of stable 1:1 M<sup>3+</sup>–H<sub>−1</sub>L<sup>2</sup> complexes with deprotonated sulfonamide N<sup>−</sup> coordination at 5 < pH < 7, on the basis of the lowered L<sup>2</sup> buffer regions (at 1 < eq(OH<sup>−</sup>) < 4) and the neutralization break at eq(OH<sup>−</sup>) = 4. In contrast, curve (d) indicated that Zn<sup>2+</sup> formed a more stable 1:1 Zn<sup>2+</sup>–L<sup>2</sup> complex without deprotonation of the sulfonamide under pH 6 and at eq(OH<sup>−</sup>) < 3. The complexation pattern is commonly shown as in Scheme

(20) The complexation of **4** with metal ions in general took more than 30 min at neutral pH. Practically, we allowed 1 h to complete the complexation.

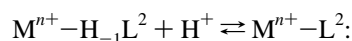
## Scheme 3



3.<sup>21</sup> The complexation constants ( $K(M-L^2)$ ) with  $Y^{3+}$ ,  $La^{3+}$ , and  $Zn^{2+}$  ions defined by Scheme 3 and eq 3 at 25 °C with  $I = 0.10$  ( $NaNO_3$ ) were determined to be 6.0 ( $Y^{3+}$ ), 5.5 ( $La^{3+}$ ), and 11.8 ( $Zn^{2+}$ ) by the program BEST,<sup>16</sup> as listed in Table 1. The protonation constants,  $K_5(M-H_{-1}L^2)$ , as defined by eq 4, are also listed in Table 1.<sup>22</sup>



$$K(M-L^2) = \frac{[M^{n+}-L^2]}{[M^{n+}][L^2]} \quad (M^{-1}) \quad (3)$$



$$K_5(M-H_{-1}L^2) = \frac{[M^{n+}-L^2]}{[M^{n+}-H_{-1}L^2]a_{H^+}} \quad (4)$$

$$K_{app}(M-H_{-1}L^2) = \frac{[M^{n+}-H_{-1}L^2]}{[M^{n+}]_{free}[L^2]_{free}}$$

$$\text{(at designated pH)} \quad (M^{-1}) \quad (5)$$

$$[L^2]_{free} = [H_3L^2]_{free} + [H_2L^2]_{free} + [HL^2]_{free} + [L^2]_{free} + [H_{-1}L^2]_{free} + [M^{n+}-L^2] \quad (6)$$

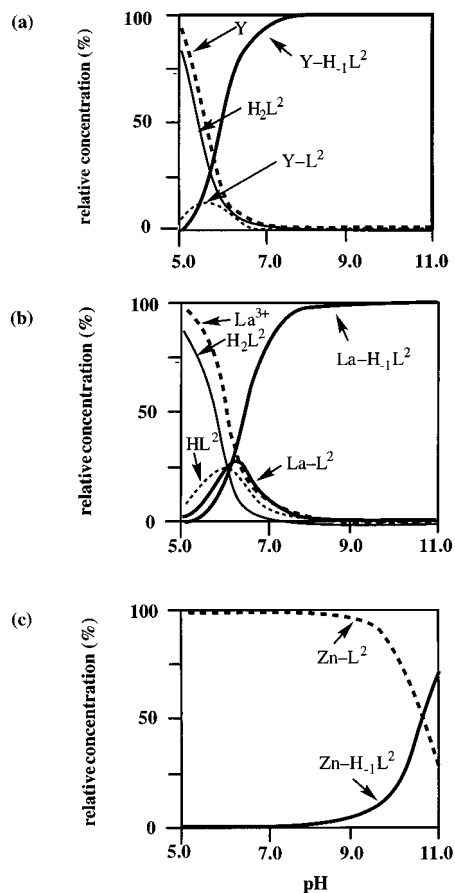
For practical understanding, an apparent complex formation constant,  $K_{app}(M-H_{-1}L^2)$ , was defined for the dansylamide-deprotonated complex,  $M^{n+}-H_{-1}L^2$ , by eqs 5 and 6, at the designated pH. The  $\log K_{app}(M-H_{-1}L^2)$  values for the  $Y^{3+}$  and  $La^{3+}$  complexes were 6.0 and 5.5, respectively, at pH 7.4. These  $\log K(M-H_{-1}L^2)$  values are smaller than that for  $La^{3+}$ -(TCMC) (10.4), although the apparent complexation constant,  $\log K(M-L^2)$ , for  $Zn^{2+}-L^2$  (11.8) is comparable to that for  $Zn^{2+}$ -(TCMC) (10.5). This may be attributed to the nature of lanthanide(III) ions, which prefer oxygen donors rather than nitrogen donors.<sup>2</sup>

Figure 6a depicts a speciation diagram for a mixture of **4** (1 mM) and  $Y^{3+}$  (1 mM) as a function of pH at 25 °C with  $I = 0.1$  ( $NaNO_3$ ), demonstrating the main population of the  $Y^{3+}-H_{-1}L^2$  complex **12a**, over 95% at pH > 6.5. Figure 6b shows that **4** forms  $La^{3+}-H_{-1}L^2$  **12b** (at  $[4] = [La^{3+}] = 1$  mM) over 95% at pH > 8. By contrast, Figure 6c shows that, at  $5 < \text{pH} < 9$ ,  $Zn^{2+}-L^2$  **11c** is the sole major species, and the deprotonation of the dansylamine did not occur, unlike the previous  $Zn^{2+}$ -**3a** complexation. The concentration of  $Zn^{2+}-L^2$  became equal to that of  $Zn^{2+}-H_{-1}L^2$  only at pH 10.7 ( $=pK_5$ ).

**The UV Spectrophotometric and Fluorometric Titration of **4** with  $La^{3+}$ ,  $Y^{3+}$ ,  $Eu^{3+}$ , and  $Zn^{2+}$ .** The interaction of metal ions with **4** at the dansylamide ( $\lambda_{max} = 330$  nm,  $\epsilon = 4.5 \times 10^3$   $M^{-1}\cdot\text{cm}^{-1}$  at pH 7.4) was examined by the UV spectrophotometric titration of **4** (0.1 mM) with metal ions ( $Fe^{2+}$ ,  $Cu^{2+}$ ,  $Zn^{2+}$ ,

(21) From the potentiometric pH titrations and X-ray crystal structure analysis of **11c** and **12a**, we concluded that no water molecule coordinates to the metal ion in **12**. The hydration state in **11** was not determined.

(22) It was reported that the  $Eu^{3+}$  and  $Tb^{3+}$  complexes of cyclens having three acetate groups and an arylsulfonamide moiety (L) have  $\log K_5(M-H_{-1}L)$  values of 5.7–6.4 (ref 13).



**Figure 6.** Speciation diagrams for the 1 mM **4** + 1 mM  $Y^{3+}$  (a), 1 mM **4** + 1 mM  $La^{3+}$  (b), and 1 mM **4** + 1 mM  $Zn^{2+}$  (c) as a function of pH at 25 °C with  $I = 0.1$  ( $NaNO_3$ ). Other species which exist at less than 5% are omitted for clarity.

$Cd^{2+}$ ,  $Al^{3+}$ ,  $Sc^{3+}$ ,  $Y^{3+}$ ,  $La^{3+}$ ,  $Eu^{3+}$ ,  $Gd^{3+}$ ,  $Tb^{3+}$ , and  $Yb^{3+}$ ) in pH 7.4 buffer (50 mM HEPES) with  $I = 0.1$  ( $NaNO_3$ ) at 25 °C. Among them,  $Fe^{2+}$ ,  $Zn^{2+}$ ,  $Cd^{2+}$ ,  $Al^{3+}$ , and  $Sc^{3+}$  (up to 2 equiv) caused little UV change. On the other hand, the UV absorption of **4** shifted to shorter wavelengths (Figure 2) upon addition of  $Cu^{2+}$ ,  $Y^{3+}$  (curve (c)),  $La^{3+}$  (curve (d)),  $Eu^{3+}$ ,  $Gd^{3+}$ ,  $Tb^{3+}$ , and  $Yb^{3+}$ , indicating their interaction with the deprotonated sulfonamide. These facts matched with the results from the potentiometric pH titrations. From the UV titration curves in Figure 7a,  $\log K_{app}(M-H_{-1}L^2)$  values were estimated to be 5.8, 5.3, and 5.1 for  $Y^{3+}$ ,  $La^{3+}$ , and  $Eu^{3+}$ , respectively, which are in reasonable agreement with the  $\log K_{app}(M-H_{-1}L^2)$  values of 6.0 and 5.2 for  $Y^{3+}$  and  $La^{3+}$ , respectively, determined earlier by the potentiometric pH titration. The  $\log K_{app}(M-H_{-1}L^2)$  values for other lanthanide(III) ions were within the range 5.8–5.1 under the same conditions.

From the fluorescence titration of **4** (Figure 7b), the  $\log K_{app}(M-H_{-1}L^2)$  values for  $Y^{3+}$ ,  $La^{3+}$ , and  $Eu^{3+}$  were determined to be 5.9, 5.4, and 5.3, respectively, which agreed reasonably well with  $\log K_{app}(M-H_{-1}L^2)$  values obtained by the UV titrations.

**X-ray Crystal Structures of  $Y^{3+}-H_{-1}L^2$  (**12a**) and  $Zn^{2+}-L^2$  Complex (**11c**).** Finally, the stable metal complexes of **4** isolated as **12a** and **11c** from pH 8 aqueous solution were characterized by X-ray crystal structure analysis.

Figure 8 is an ORTEP drawing of the  $Y^{3+}-H_{-1}L^2$  **12a**. The dansylamide is certainly deprotonated to coordinate to the  $Y^{3+}$  ion. In total,  $Y^{3+}$  is nine-coordinate, with four nitrogen atoms of the cyclen ring, carbonyl oxygens of three carbamoylmethyl

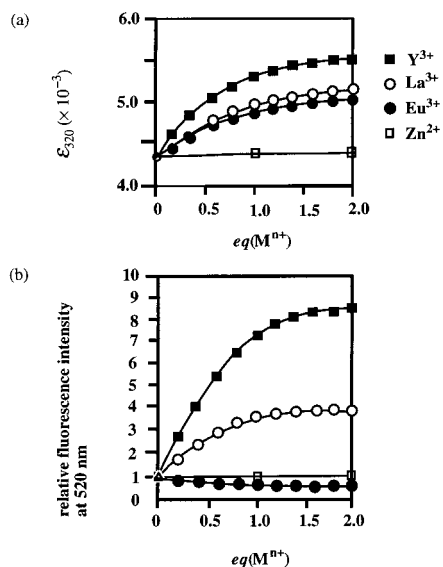


**Figure 7.** UV titration curves (a) and fluorescence titration curves (b) of **4** with  $Zn^{2+}$  (white squares),  $Y^{3+}$  (black squares),  $La^{3+}$  (white circles), and  $Eu^{3+}$  (black circles) at 25 °C and pH 7.4 (50 mM HEPES for UV titration and 10 mM HEPES for fluorescence titration) with  $I = 0.1$  ( $NaNO_3$ ) ( $[4] = 0.1$  mM for UV titration and  $[4] = 10$   $\mu$ M for fluorescence titration).  $eq(M^{n+})$  is the number of equivalents of metal added against **4**.

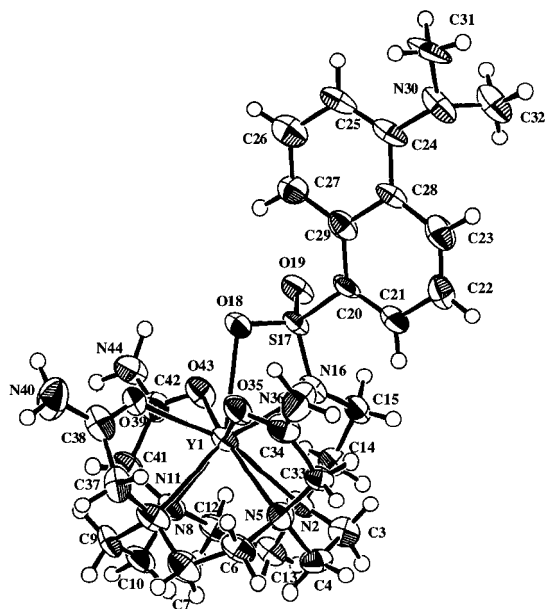


**Figure 8.** ORTEP drawings (50% probability ellipsoids) of  $Y^{3+}$ - $H_{-1}L^2$  complex **12a**. All external nitrates and water molecules are omitted for clarity. Selected bond distances (Å): Y1–N2 2.616(8), Y1–N5 2.633(8), Y1–N8 2.606(8), Y1–N11 2.613(7), Y1–N16 2.342(7), Y1–O18 2.589(6), Y1–O35 2.365(7), Y1–O39 2.298(6), Y1–O43 2.329(8). Selected bond angles (deg): O18–Y1–O35 67.1(2), O18–Y1–O39 72.9(2), O18–Y1–O43 70.5(2), O18–Y1–N2 121.3(2), O18–Y1–N5 121.5(2), O18–Y1–N8 133.7(2), O18–Y1–N11 133.5(2), O18–Y1–N16 56.7(2), N2–Y1–N5 68.5(2), N2–Y1–N8 104.6(2), N2–Y1–N11 68.8(2), N2–Y1–N16 65.8(2), O18–S17–N16 103.3(4), O19–S17–N16 116.3(4).

parts, one sulfonyl oxygen, and the  $N^-$  of the sulfonamide, whereby  $Y^{3+}$  has a square antiprismatic coordination geometry. The  $Y^{3+}$ - $N^-$  (dansylamide anion) bond length is 2.34 Å, which is longer than the  $Zn^{2+}$ - $N^-$  distance of 1.97 Å in  $Zn^{2+}$ - $H_{-1}L^1$  **3b**. The average  $Y^{3+}$ - $N$ (cyclen) bond lengths and  $Y^{3+}$ - $O$ (carbonyl) bond lengths are 2.62 and 2.33 Å, respectively,

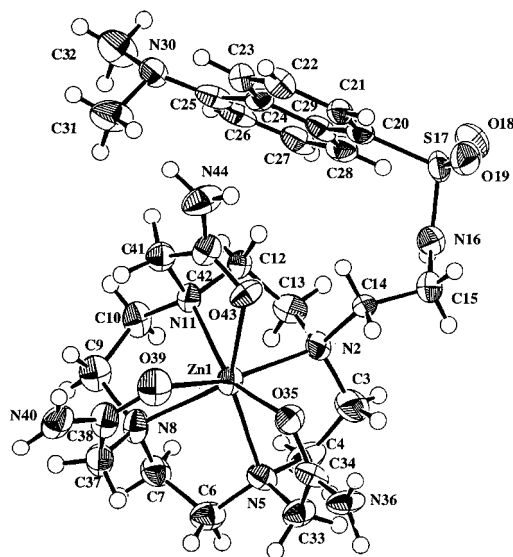


**Figure 9.** ORTEP drawings (50% probability ellipsoids) of  $Zn^{2+}$ - $L^2$  complex **11c**. All external nitrates and water molecules are omitted for clarity. Selected bond distances (Å): Zn1–N2 2.321(6), Zn1–N5 2.328(7), Zn1–N8 2.353(7), Zn1–N11 2.221(6), Zn1–O35 2.071(5), Zn1–O39 2.235(5), Zn1–O43 2.214(5). Selected bond angles (deg): O35–Zn1–O39 84.5(2), O35–Zn1–O43 79.8(2), O35–Zn1–N2 90.2(2), O35–Zn1–N5 76.8(2), O35–Zn1–N8 128.1(2), O35–Zn1–N11 152.5(2), O39–Zn1–O43 75.4(2), O39–Zn1–N2 161.6(2), O39–Zn1–N5 116.4(2), O39–Zn1–N8 71.2(2), O39–Zn1–N11 98.3(2), O43–Zn1–N2 86.4(2), O43–Zn1–N5 152.3(2), O43–Zn1–N8 132.4(2), O43–Zn1–N11 74.5(2), N2–Zn1–N5 79.2(2), N2–Zn1–N8 124.8(2), N2–Zn1–N11 78.5(2), N5–Zn1–N8 74.6(2), N5–Zn1–N11 124.5(2), N8–Zn1–N11 77.9(2).

which are comparable to 2.64 Å for  $Eu^{3+}$ - $N$ (cyclen) and 2.39 Å for  $Eu^{3+}$ - $O$ (carbonyl) in nine-coordinate  $[Eu-(TCMC)-(H_2O)]^{3+}$  **13**.<sup>6c</sup> In an homologous nine-coordinate  $Tb^{3+}$  complex **14**, the average  $Tb^{3+}$ - $N$ (cyclen) and  $Tb^{3+}$ - $O$ (carbonyl) bond lengths are 2.69 and 2.35 Å, respectively.<sup>17</sup> As a result of the coordination of three carbonyl oxygens (due to the swirl of the pendant groups) and one of the two sulfonyl oxygens to the  $Y^{3+}$  ion ( $Y^{3+}$ - $O$  bond is 2.56 Å), **11** is a chiral molecule. In a unit cell, both enantiomers are included. In  $Zn^{2+}$ - $H_{-1}L^1$  **3b**, the sulfonyl oxygen did not bind to  $Zn^{2+}$ .

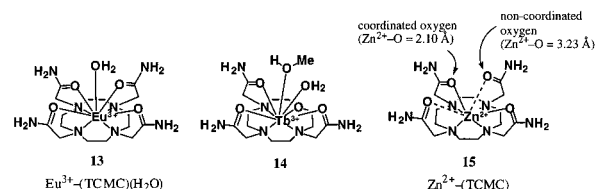
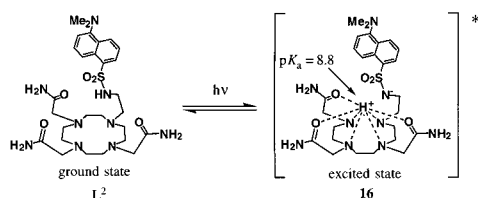


Figure 9 shows an ORTEP drawing of the  $Zn^{2+}$ - $L^2$  **11c**. It is now unequivocally proven that the dansylamide proton is not bound to  $Zn^{2+}$ , and hence it locates off the cyclen ring with the naphthalene ring almost perpendicular to the cyclen face. Zinc(II) is seven-coordinate with four nitrogens of the cyclen ring (the average  $Zn^{2+}$ - $N$  bond is 2.31 Å) and three carbonyl oxygens of carbamoylmethyls (the average  $Zn^{2+}$ - $O$  bond is 2.17 Å). For comparison, in the complex **3b**, the average  $Zn^{2+}$ - $N$ (cyclen) bond length was 2.13 Å. Four nitrogens of the cyclen ring and the  $Zn^{2+}$  ion form a tetragonal pyramid, and three oxygens of carbamoylmethyls and  $Zn^{2+}$  form a trigonal pyramid in **11c**.<sup>23</sup> In a reported  $Zn^{2+}$ - $(TCMC)$  complex **15**,  $Zn^{2+}$  is six-coordinate with an average  $Zn^{2+}$ - $N$  distance of 2.25 Å.<sup>27b</sup> Although the two orthogonal carbonyl oxygens coordinated to

**Table 2.** Selected X-ray Crystal Data for the  $Y^{3+}$  Complex **12a** and the  $Zn^{2+}$  Complex **11c**

	<b>12a</b>	<b>11c</b>
formula	$C_{28}H_{49}N_{11}O_{13.5}SY$	$C_{28}H_{51}N_{11}O_{14}SZn$
$M_r$	876.73	863.22
cryst syst	monoclinic	monoclinic
space group	$P2_1/c$ (No. 14)	$C2/c$ (No. 15)
$a$ (Å)	18.912(3)	35.361(1)
$b$ (Å)	17.042(3)	13.7298(5)
$c$ (Å)	24.318(4)	18.5998(6)
$\beta$ (deg)	95.99(1)	119.073(2)
$V$ (Å <sup>3</sup> )	7794(2)	7892.3(5)
$Z$	8	8
$D_{calc}$ (g·cm <sup>-3</sup> )	1.494	1.453
$\mu$ (Mo(K $\alpha$ )) (cm <sup>-1</sup> )	$\mu$ (Cu K $\alpha$ ) = 32.69	$\mu$ (Mo K $\alpha$ ) = 7.52
$R1$ ( $\sum   F_o  -  F_c   / \sum  F_o $ )	0.160	0.084
no. of reflectns used for calculation of $R1$ ( $I > 2\sigma(I)$ )	7140	6125
no. of variables	887	438

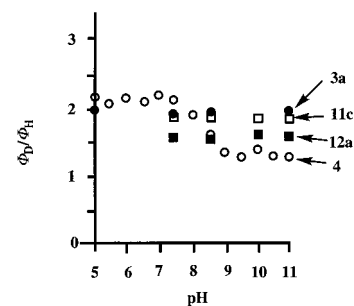
**Scheme 4**

$Zn^{2+}$  (the average  $Zn^{2+}-O$  length is 2.10 Å) and the other two carbonyl oxygens remained uncoordinated ( $Zn^{2+}-O$  length is 3.23 Å) in the solid state, it is estimated that the rapid interconversion from one pair of  $Zn^{2+}-O$  bonds long and the other pair short to the opposite arrangement would proceed through a more regular structure with all  $Zn^{2+}-O$  bonds equivalent.<sup>7b</sup> Typical crystal data for **12a** and **11c** are listed in Table 2.

**Discussion**

Our newly designed doubly functionalized cyclen with three carbamoylmethyl groups and a fluorescent dansylamide pendant **4** has two novel properties of the dansylamide fluorescence by itself and by metal complexes in comparison with those of the predecessor lacking the carbamoylmethyls, **3a**.

First, as disclosed by Figure 3b, the fluorescence of uncomplexed **4** itself was remarkably enhanced above pH 8 in aqueous solution, while that of **3a** increased only a little above pH 11. For **4**, the pH-dependent intensity of the fluorescence gave a  $pK_a$  of  $8.8 \pm 0.2$  (Figure 3b), which is closed to the  $\log K_2$  of 8.4 for  $L^2 + H^+ \rightleftharpoons (HL^2)^+$  in Scheme 2. We were thus led to conclude that emerging nonprotonated  $L^2$  above pH 8 is responsible for the intensified emission (Figure 4b). We then postulated that the intensified fluorescence of **4** above pH 8 may be derived from the polarized structure in the excited state **16**, as depicted in Scheme 4, where three carbamoylmethyls become available for the proton abstraction from the dansylamide. The  $pK_a$  value of 8.8 was thus assigned to the dansylamide deprotonation in the excited state. For **3a**, the fluorescence titration gave a  $pK_a$  value of 10.8 (Figure 3b), the same as the value determined for the ground state by the potentiometric pH titration. It was earlier reported that the  $\Phi_D/\Phi_H$  value for 5-amino-1-naphthalenesulfonate containing an amino group as a proton donor is 3.07 ( $\Phi_D$  and  $\Phi_H$  are the quantum yields of

**Figure 10.** pH-dependent change of quantum yield ratios ( $\Phi_D/\Phi_H$ ) of **3a** (black circles), **4** (white circles), **11c** (white squares), and **12a** (black squares) at 25 °C ( $[3a] = [4] = [11c] = [12a] = 10 \mu M$ ).

the fluorescence emission in  $D_2O$  and  $H_2O$ , respectively), while that for 1-naphthalenesulfonate containing no proton donor is ca. 1.<sup>24</sup> These results were interpreted as an isotope effect on the rate of proton transfer during the excited-state lifetime. This technique was applied to check the postulated polarized structure **16**. The  $\Phi_D/\Phi_H$  values for **3a**, **4**, **11c**, and **12a** (all 10  $\mu M$ ) in  $D_2O$  and  $H_2O$  were determined at various pH values, as plotted in Figure 10. The values for **3a** stayed at ca. 2 at pH 5–11, and those for **11c** and **12a** were ca. 1.9 and ca. 1.6, respectively. In contrast, the  $\Phi_D/\Phi_H$  values for **4** changed from 2.2 at lower pH to 1.4 at higher pH with a tentative  $pK_a$  value of ca. 8, a fact supporting the notion (Scheme 4) that the dansylamide is a protonated form ( $ArSO_2NHR$ ) at lower pH and a deprotonated form ( $ArSO_2N^-R$ ) at higher pH in the excited state.<sup>25</sup>

The second point is the different fluorescent responses to metal ions by **3a** and **4**. The preceding compound **3a** sensed  $Zn^{2+}$  (and  $Cd^{2+}$ ) by strong fluorescent emission but did not sense lanthanide(III) ions such as  $Y^{3+}$  and  $La^{3+}$ . The large (4.9 times) fluorescence enhancement of **3a** (at 528 nm when excited at 330 nm) with a subnanomolar concentration of zinc(II) ion (at pH 7.3) was ascribed to the deprotonated dansylamide moiety coordinating to  $Zn^{2+}$  as a fifth ligand from an apical site. Since lanthanide(III) ions hardly bound to **3a**, **3a** did not act as a probe for  $Y^{3+}$  and  $La^{3+}$ . In contrast, the present **4** bound both to  $Zn^{2+}$  (as **11c**) and to lanthanide(III) ions (as **12**) at pH 7.4. The apparent 1:1 complexation constant for **11c**,  $\log K_{app}(Zn-L^2)$ ,<sup>26</sup> at pH 7.4 is 10.9, and  $\log K_{app}(M-H-L^2)$  values at pH 7.4 for **12a** and **12b** are 6.0 and 5.2 (Table 1), respectively. Therefore, the  $Zn^{2+}$  complex is more stable than the lanthanide(III) complexes in neutral pH solution. The  $Zn^{2+}$  is already saturated with seven donors of **4** (four from cyclen N's and three from carbonyl O's) and no longer bothers with further coordination with the sulfonamide (see Figure 7a) to stay as  $Zn^{2+}-L^2$  **11c**. One may also describe that three carbamoyl oxygens bind simultaneously to  $Zn^{2+}$  to mask the acidity of the  $Zn^{2+}$  ion, which prevented the coordination of the dansyl unit. Deprotonation of the dansylamide in **11c** occurred only at pH > 11 with a little enhancement of emission (Figure 5). Since its  $pK_a$  of 10.7 is close to the value of 10.6 for the free ligand (Scheme 2),  $Zn^{2+}$  may not bind to it, unlike the tentative description of

(24) Stryer, L. *J. Am. Chem. Soc.* **1966**, *88*, 5708–5712.(25) Negligible phosphorescence was observed for **4**, **11c**, and **12a** (excitation at 335 nm) at the employed concentration of 10  $\mu M$ , pH 7.4, and 25 °C.(26) The apparent 1:1 complexation constant of **4** with  $Zn^{2+}$ ,  $K_{app}(Zn-L^2)$ , is defined by eqs 7 and 8.

$$K_{app}(Zn-L^2) = [(Zn^{2+}-H-L^2) + (K_{app}(Zn-L^2) = [(Zn^{2+}-H-L^2) + (Zn^{2+}-L^2)]/[Zn^{2+}]_{free}[L^2]_{free} \quad (\text{at designated pH}) \quad (M^{-1}) \quad (7)$$

$$[L^2]_{free} = [H_3L^2]_{free} + [H_2L^2]_{free} + [HL^2]_{free} + [L^2]_{free} + [H-L^2]_{free} \quad (8)$$

(23) In the crystal packing, the naphthyl rings of two dansyl units are placed face to face in an intermolecular manner (see the Supporting Information).

**12c** in Scheme 3. As a consequence, **4** could not be a fluorophore for  $Zn^{2+}$  (Figures 5 and 7b). On the other hand, more acidic and bigger lanthanide(III) ions extend their acidities to the remote donor, even in the nine-coordinating complexes.<sup>1,2,27</sup> The resulting deprotonated dansylamides in **12a** and **12b** were responsible for  $Y^{3+}$  and  $La^{3+}$  sensings with **4** (Figure 5 and 7b).<sup>28,29</sup> Other lanthanide(III) ions also formed 1:1 complexes with similar complexation constants such as **12a** and **12b**, as concluded from the UV spectrophotometric titrations (for  $Eu^{3+}$ , Figure 7a).<sup>30</sup> However, all other lanthanide(III) ions with unfilled f-orbitals quenched the dansyl fluorescence (Figures 5 and 7b).<sup>31</sup> Likewise, the  $d^9$   $Cu^{2+}$  complex quenched the emission (Figures 5 and 7b).

## Conclusions

The double functionalization of a cyclen with a dansyl group and three carbamoylmethyl moieties, **4**, dramatically expanded the fluorescence behaviors of a cyclen in comparison with **3a**. The three-carbamoyl functionalization provided the hydrogen-bonding donors to facilitate the nearby dansyl deprotonation to accompany strong fluorescent emission in the excited state. The appended three carbamoyls stabilized yttrium(III)- and lanthanum(III)-cyclen complexes to permit selective and efficient signaling from the deprotonated dansyl group. Cyclen derivatives such as **4** may be a convenient and selective sensor for qualitative and quantitative assays of micromolar concentrations of  $Y^{3+}$  and  $La^{3+}$  ions in water solutions. Sensing of  $Y^{3+}$ , which is an important metal ion in radioimmunotherapy ( $^{90}Y$ ),<sup>4</sup> should be clinically useful.<sup>32</sup>

## Experimental Section

**General Information.** All reagents and solvents used were of the highest commercial quality and used without further purification.  $Sc(NO_3)_3 \cdot 4H_2O$ ,  $Y(NO_3)_3 \cdot 6H_2O$ ,  $La(NO_3)_3 \cdot 6H_2O$ ,  $Eu(NO_3)_3 \cdot 4H_2O$ , and  $Tb(NO_3)_3 \cdot 6H_2O$  were purchased from Soekawa Co. Ltd., and  $Gd(NO_3)_3 \cdot 6H_2O$  and  $Yb(NO_3)_3 \cdot 4H_2O$  were purchased from Wako Pure Chemical Industries, Co. Ltd. The purity of these metals was checked by EDTA-Arsenazo III (Dojin Chemical Co. Ltd.) titration. All aqueous solutions were prepared using deionized and redistilled water. Buffer (50 mM) solutions (CAPS, pH 12.0, 11.5, 11.0, 10.5, and 10.0; CHES, pH 9.5, 9.3, 9.0, and 8.8; TAPS, pH 8.5; EPPS, pH 8.0; HEPES, pH 7.0 and

(27) Nash, K. L. In *Handbook on the Physics and Chemistry of Rare Earths*; Gschneidner, K. A., Jr., Eyring, L., Choppin, G. R., Lander, G. H., Eds.; North-Holland: Amsterdam, 1994; Vol. 18, pp 197–238.

(28) The  $^1H$  NMR (500 MHz) experiments on **4** and its complexes with  $Y^{3+}$  and  $Zn^{2+}$  in  $D_2O$  at pD 7.0 and 11.0 (at 35 °C) showed good agreement with their deprotonation behavior (see the Supporting Information). Above a  $pK_a$  of 10.8, the dansylamide of **4** is deprotonated and the  $H_{2'}$  signal (for assignment, see Scheme 3 and ref 19) moved upfield by 0.2 ppm. The  $H_{2'}$  signal of  $Zn^{2+}-L^2$  **11c** moved similarly upfield at pD 12.0. The  $H_{2'}$  signal of  $Y^{3+}-H_{-1}L^2$  **12a** at pD 7.0 appeared more upfield at  $\delta$  7.94. The  $H_{2'}$ ,  $H_{4'}$ , and  $H_{8'}$  signals of  $La^{3+}-H_{-1}L^2$  **12b** at pD 7.0 were broadened, possibly due to the presence of somewhat slow equilibration between several conformers.

(29) The metal complexes **11c**, **12a**, and **12b** were kinetically fairly inert. Because the  $Zn^{2+}$  complex **11c** is thermodynamically more stable than the lanthanide(III) complexes **12a** and **12b**, the fluorescence intensity of **12a** decreased by 25% after addition of 5 equiv of  $Zn^{2+}$  in 2 days at 25 °C.

(30) The fluorescence of **4** did not respond to  $Sc^{3+}$  (Figure 4). By the potentiometric pH titration, the  $\log K_{app}(M-L^2)$  and  $pK_5(M-H_{-1}L^2)$  values for the  $Sc^{3+}$  complex of **4** were determined to be 9.2 and 9.8, implying that dansylamide is scarcely deprotonated at neutral pH.

(31) As pointed out by reviewers, other rare earth metal ions interfere with  $Y^{3+}$  and  $La^{3+}$  sensing by **4**.

(32) For reviews on Y(III) and La(III) complexes, see: (a) Hart, F. A. In *Comprehensive Coordination Chemistry*; Wilkinson, G. W., Gillard, R. D., McCleverty, J. A., Eds.; Pergamon Press: Oxford, 1987; Vol. 3, pp 1059–1127. (b) Sessler, J. L.; Mody, T. D.; Hemmi, G. W.; Lynch, V. *Inorg. Chem.* **1993**, *32*, 3175–3187. (c) Sessler, J. L.; Hemmi, G.; Mody, T. D.; Murai, T.; Murrell, A.; Young, S. W. *Acc. Chem. Res.* **1994**, *27*, 43–50.

7.4; and MES, pH 6.5, 6.0, 5.5, and 5.0) were used, and the ionic strengths of all were adjusted to 0.10 with  $NaNO_3$ . The Good's buffers ( $pK_a$  at 20 °C) were purchased from Dojindo and were used without further purification: CAPS (3-(cyclohexylamino)propanesulfonic acid, 10.4), CHES (2-(3-cyclohexylamino)-2-hydroxypropanesulfonic acid, 9.0), TAPS (3-[N-tris(hydroxymethyl)methylamino]propanesulfonic acid, 8.1), EPPS (3-(4-(2-hydroxyethyl)-1-piperazinyl)propanesulfonic acid, 8.0), HEPES (2-(4-(2-hydroxyethyl)-1-piperazinyl)ethanesulfonic acid, 7.6), and MES (2-morpholinoethanesulfonic acid, 6.2). Melting points were measured on a Yanaco melting point apparatus and listed without correction. IR spectra were recorded on a Shimadzu FTIR-4200 spectrometer.  $^1H$  NMR spectra were recorded on a JEOL Delta (500 MHz) or Alpha (400 MHz) spectrometer. Tetramethylsilane (TMS) in  $CDCl_3$  and  $CD_3OD$  and 3-(trimethylsilyl)propionic-2,2,3,3- $d_4$  acid sodium salt (TSP) in  $D_2O$  were used as internal or external references for  $^1H$  NMR measurements, respectively. 1,4-Dioxane was used as an internal or external reference for  $^{13}C$  NMR in  $D_2O$ . The pD values in  $D_2O$  were corrected for a deuterium isotope effect using  $pD = [pH\text{-meter reading}] + 0.40$ . Elemental analysis was performed on a Perkin-Elmer CHN Analyzer 2400. Thin-layer chromatography (TLC) and silica gel column chromatography were performed using a Merck Art. 5554 (silica gel) TLC plate and Fuji Silysia Chemical FL-100D (silica gel), respectively.

**1-Benzoyloxycarbonyl-1,4,7,10-tetraazacyclododecane Trihydrochloride Salt (7·3HCl·2H<sub>2</sub>O).** Benzyl chloroformate (2.8 g, 16.0 mmol) was added to a mixture of 1,4,7-tris(*tert*-butyloxycarbonyl)-1,4,7,10-tetraazacyclododecane (**5**) (6.4 g, 13.5 mmol)<sup>15</sup> and triethylamine (1.6 g, 16.0 mmol) in  $CHCl_3$  (100 mL) at 0 °C, and the whole was stirred at room temperature for 8 h. An insoluble material was filtered off, and the reaction mixture was concentrated under reduced pressure. The remaining residue was purified by silica gel column chromatography (eluent: hexane/AcOEt) to yield **6** as a colorless amorphous solid (7.8 g).

A colorless solution of **6** (7.8 g, 12.8 mmol) and concentrated HCl (10 mL) in MeOH (60 mL) was stirred overnight at room temperature. The precipitated powders were filtered and recrystallized from THF/ $H_2O$  to yield **7·3HCl·2H<sub>2</sub>O** as colorless powders (4.4 g, 72% yield): TLC ( $CH_2Cl_2$ /MeOH/aqueous 28%  $NH_3 = 10:4:1$ ):  $R_f = 0.4$ . Mp 178–180 °C. IR (KBr): 3566, 3417, 3008, 2948, 2807, 1709, 1670, 1616, 1475, 1447, 1423, 1250, 1145, 732, 706  $cm^{-1}$ .  $^1H$  NMR (400 MHz,  $D_2O$ /TSP):  $\delta$  3.18–3.23 (12H, m,  $NCH_2$ ), 3.70–3.73 (4H, m,  $NCH_2$ ), 5.21 (2H, s,  $PhCH_2O$ ), 7.45–7.48 (5H, m,  $ArH$ ).  $^{13}C$  NMR (100 MHz,  $D_2O$ /1,4-dioxane):  $\delta$  43.79, 45.57, 46.23, 47.53, 69.54, 129.31, 129.74, 129.84, 136.64, 159.39. Anal. Calcd for  $C_{16}H_{33}N_4O_4Cl_3$ : C, 42.53; H, 7.36; N, 12.40. Found: C, 42.54; H, 7.66; N, 12.37.

**2-(5-(Dimethylamino)-1-naphthalenesulfonylamido)ethyl Chloride (10).** A  $CHCl_3$  (35 mL) solution of dansyl chloride (2-(5-(dimethylamino)-1-naphthalene)sulfonyl chloride) (11.6 g, 43 mmol) was added dropwise to a mixture of 2-chloroethylamine (5.0 g, 43 mmol) and triethylamine (8.7 g, 86 mmol) in  $CHCl_3$  (100 mL) at room temperature. After being stirred overnight, the reaction mixture was washed with saturated aqueous  $NaHCO_3$ , 10% aqueous citric acid, and saturated aqueous NaCl. The organic layer was dried with  $K_2CO_3$ , filtered, and concentrated in vacuo. The remaining powders were recrystallized from AcOEt to yield **10** (7.2 g, 54%): TLC (hexane/AcOEt = 2:1):  $R_f = 0.5$ . Mp 100–102 °C dec. IR (KBr): 3271, 2955, 2832, 2790, 2361, 2337, 1435, 1307, 1136, 1084, 922, 799, 630, 561  $cm^{-1}$ .  $^1H$  NMR (500 MHz,  $CDCl_3$ /TMS):  $\delta$  2.87 (6H, s,  $N(CH_3)_2$ ), 3.23 (2H, dt,  $NCH_2CCH_2Cl$ ,  $J = 5.6, 6.4$  Hz), 3.47 (2H, t,  $CCH_2Cl$ ,  $J = 5.6$  Hz), 5.11 (1H, t-like,  $NH$ ), 7.18 (1H, d,  $ArH$  ( $H_{6'}$ ),  $J = 7.6$  Hz), 7.51 (1H, dd,  $ArH$  ( $H_{3'}$ ),  $J = 6.4, 8.8$  Hz), 7.57 (1H, dd,  $ArH$  ( $H_{7'}$ ),  $J = 7.6, 8.4$  Hz), 8.23 (2H, d,  $ArH$  ( $H_{4'}$ ),  $J = 6.4$  Hz), 8.26 (1H, d,  $ArH$  ( $H_{8'}$ ),  $J = 8.4$  Hz), 8.56 (1H, d,  $ArH$  ( $H_{2'}$ ),  $J = 8.8$  Hz).  $^{13}C$  NMR (100 MHz,  $CHCl_3$ ):  $\delta$  43.65, 44.76, 45.39, 115.36, 118.53, 123.12, 128.62, 129.54, 129.58, 129.98, 130.82, 134.52, 152.13. Anal. Calcd for  $C_{14}H_{17}N_2O_2S$ : C, 53.76; H, 5.48; N, 8.96. Found: C, 53.85; H, 5.45; N, 9.10.

**1-(2-(5-(Dimethylamino)-1-naphthalenesulfonylamido)ethyl)-4,7,10-tris(carbamoylmethyl)-1,4,7,10-tetraazacyclododecane Trihydrochloride Salt (4·3HCl·2H<sub>2</sub>O).** The acid-free **7** was obtained by extraction of **7·3HCl·2H<sub>2</sub>O** (2.7 g, 5.9 mmol) with  $CHCl_3$  from 1 N



NaOH. The resulting free **7** was dissolved in 30 mL of MeCN and stirred overnight with 2-bromoacetamide (3.4 g, 25 mmol) in the presence of anhydrous  $K_2CO_3$  (3.0 g, 22 mmol) under reflux temperature. An insoluble material was filtered off, and the reaction mixture was concentrated under reduced pressure. The remaining residue was purified by silica gel column chromatography ( $CH_2Cl_2/MeOH$ ) to yield **8** as a colorless oil (1.5 g). TLC ( $CH_2Cl_2/MeOH/aqueous\ 28\%\ NH_3 = 10:4:1$ ):  $R_f = 0.5$ .  $^1H\ NMR$  (400 MHz,  $CDCl_3/TMS$ ):  $\delta$  2.60–2.65 (8H, m,  $NCH_2$ ), 2.85–3.02 (4H, m,  $NCH_2$ ), 3.06–3.15 (6H, m,  $NCH_2$ ), 3.49 (4H, brs,  $NCH_2CONH_2$ ), 5.10 (2H, s,  $PhCH_2O$ ), 5.89 (2H, br,  $NCH_2CONH_2$ ), 7.05–7.16 (2H, br,  $NCH_2CONH_2$ ), 7.32–7.36 (5H, m,  $ArH$ ).

A mixture of **8** (1.5 g) and 10% palladium-on-carbon (0.2 g) in THF/MeOH (1:1) was stirred vigorously under 1 atm of  $H_2$  overnight at room temperature. The mixture was filtered through Celite (No. 545) with THF/MeOH to afford **9** as a colorless amorphous solid (1.0 g). TLC ( $CH_2Cl_2/MeOH/aqueous\ 28\%\ NH_3 = 10:4:1$ ):  $R_f = 0.1$ .  $^1H\ NMR$  (400 MHz,  $CD_3OD/TMS$ ):  $\delta$  2.49 (4H, s,  $NCH$ ), 2.56 (8H, m,  $NCH_2$ ), 3.04 (2H, s,  $NCH_2CONH_2$ ), 3.08 (4H, s,  $NCH_2CONH_2$ ).  $^{13}C\ NMR$  (100 MHz,  $CD_3OD/TMS$ ):  $\delta$  44.76, 51.19, 56.29, 56.65, 57.73, 175.16, 175.39.

A mixture of crude **9** (1.0 g), **10** (920 mg, 1.8 mmol), and  $K_2CO_3$  (1.0 g, 2.6 mmol) in MeOH (70 mL) was stirred overnight under reflux temperature. After the mixture cooled, an insoluble material was filtered off, and the reaction mixture was concentrated under reduced pressure. The remaining residue was purified by silica gel column chromatography ( $CH_2Cl_2/MeOH$ ) to yield **4** as a colorless amorphous solid (0.92 g).

The free **4** (0.92 g) was dissolved in MeOH (30 mL), and concentrated HCl (5 mL) was added at 0 °C. After being stirred for 10 min, the reaction mixture was evaporated in vacuo, and the remaining powders were recrystallized from EtOH/MeOH to yield  $4 \cdot 3HCl \cdot 2H_2O$  as colorless prisms (0.72 g, 16% from  $7 \cdot 3HCl \cdot 2H_2O$ ). Mp 213–215 °C dec. IR (KBr): 3523, 1672, 1622, 1469, 1440, 1324, 1143, 1089, 794, 670, 347, 586  $cm^{-1}$ .  $^1H\ NMR$  (500 MHz,  $D_2O/TSP$ ):  $\delta$  2.98–3.68 (26H, m,  $CH_2$ ), 2.58–2.85 (16H, m,  $CH_2$ ), 2.91 (6H, s,  $N(CH_3)_2$ ), 3.19 (8H, brs,  $CH_2$ ), 7.46 (1H, d,  $ArH(6')$ ,  $J = 7.2\ Hz$ ), 7.72–7.77 (2H, two dd,  $ArH(3')$  &  $ArH(7')$ ), 8.31 (2H, two d,  $ArH(2')$  &  $ArH(8')$ ), 8.56 (1H, d,  $ArH(4')$ ,  $J = 8.8\ Hz$ ).  $^{13}C\ NMR$  (100 MHz,  $D_2O/1,4$ -dioxane):  $\delta$  38.41, 47.35, 50.12, 50.26, 50.64, 53.44, 55.20, 55.79, 119.98, 125.94, 127.14, 127.38, 127.70, 129.34, 129.47, 131.40, 135.05, 141.49, 180.37, 180.65. Anal. Calcd for  $C_{28}H_{52}N_9O_7SCl_3$ : C, 43.95; H, 6.85; N, 16.47. Found: C, 43.95; H, 7.05; N, 16.25.

**1-(2-(5-(Dimethylamino)-1-naphthalenesulfonylamido)ethyl)-4,7,10-tris(carbamoylmethyl)-1,4,7,10-tetraazacyclododecane  $Y^{3+}$  Complex ( $Y^{3+}-H_{-1}L^2 \cdot 2(NO_3^-) \cdot 3H_2O$ ) (**12a**).**  $5 \cdot 3Cl \cdot 2H_2O$  (122 mg, 0.16 mmol),  $Y(NO_3)_3 \cdot 6H_2O$  (74 mg, 0.19 mmol), and  $NaNO_3$  (0.85 g, 10 mmol) were dissolved in  $H_2O$ , and the pH was adjusted to pH 8.0 with aqueous NaOH. This aqueous solution was concentrated slowly under a reduced pressure at room temperature for 1 week, and  $Y^{3+}-H_{-1}L^2 \cdot 2(NO_3^-) \cdot 3H_2O$  (**12a**) was obtained as colorless prisms (61 mg, 43%). Mp > 250 °C dec (turns yellow at 160 °C). IR (KBr): 3395, 2873, 1668, 1607, 1474, 1459, 1385, 1339, 1224, 1177, 1082, 918, 810, 669, 629  $cm^{-1}$ .  $^1H\ NMR$  (500 MHz,  $D_2O/TSP$ ):  $\delta$  2.2–3.9 (26H, brm,  $CH_2$ ), 2.92 (6H, s,  $N(CH_3)_2$ ), 7.45 (1H, d,  $ArH(6')$ ,  $J = 7.6\ Hz$ ), 7.62 (1H, dd,  $ArH(3')$ ,  $J = 7.2, 8.8\ Hz$ ), 7.71 (1H, dd,  $ArH(7')$ ,  $J = 7.6, 8.0\ Hz$ ), 7.94 (1H, d,  $ArH(2')$ ,  $J = 7.2\ Hz$ ), 8.35 (1H, d,  $ArH(8')$ ,  $J = 8.0\ Hz$ ), 8.38 (1H, d,  $ArH(4')$ ,  $J = 8.8\ Hz$ ).  $^{13}C\ NMR$  (100 MHz,  $D_2O/1,4$ -dioxane):  $\delta$  46.45, 117.53, 122.27, 125.54, 126.48, 129.50, 130.10, 130.39, 132.24, 135.27, 141.84, 178.99, 180.12 ( $^{13}C$  signals of cyclen moiety and side chains except the dansyl unit were hardly observed). Anal. Calcd for  $C_{28}H_{50}N_{11}O_{14}SY$ : C, 37.97; H, 5.69; N, 17.40. Found: C, 37.79; H, 5.65; N, 17.12.

**1-(2-(5-(Dimethylamino)-1-naphthalenesulfonylamido)ethyl)-4,7,10-tris(carbamoylmethyl)-1,4,7,10-tetraazacyclododecane  $Zn^{2+}$  Complex ( $Zn^{2+}-L^2 \cdot 2(NO_3^-) \cdot 3.5H_2O$ ) (**11c**).**  $5 \cdot 3HCl \cdot 2H_2O$  (152 mg, 0.20 mmol),  $ZnSO_4 \cdot 7H_2O$  (63 mg, 0.22 mmol), and  $NaNO_3$  (174 mg, 2.0 mmol) were dissolved in  $H_2O$ , and the pH was adjusted to pH 8.0 with aqueous NaOH. This aqueous solution was concentrated slowly under a reduced pressure at room temperature for 1 week, and  $Zn^{2+}-L^2 \cdot 2(NO_3^-) \cdot 3.5H_2O$  (**11c**) was obtained as yellow prisms (91 mg, 52%).

Mp 194–196 °C dec. IR (KBr): 3354, 3154, 2947, 2872, 1698, 1676, 1653, 1456, 1384, 1325, 1142, 1095, 1021, 943, 803  $cm^{-1}$ .  $^1H\ NMR$  (500 MHz,  $D_2O/TSP$ ):  $\delta$  2.25–2.32 (2H, m,  $CH_2$ ), 2.36–2.45 (2H, m,  $CH_2$ ), 2.51 (2H, t-like, dansyl- $NCH_2CH_2N$ ), 2.58–2.72 (8H, m,  $CH_2$ ), 2.86–2.97 (2H, m,  $CH_2$ ), 2.90 (6H, brs,  $N(CH_3)_2$ ), 2.96–3.08 (2H, m,  $CH_2$ ), 3.11 (2H, t-like, dansyl- $NCH_2CH_2N$ ), 3.29 (2H, d,  $CH_2CONH_2$ ,  $J = 17.2\ Hz$ ), 3.41 (2H, s,  $CH_2CONH_2$ ), 3.59 (2H, d,  $CH_2CONH_2$ ,  $J = 17.2\ Hz$ ), 7.46 (1H, d,  $ArH(6')$ ,  $J = 7.6\ Hz$ ), 7.71–7.76 (2H, two d,  $ArH(3')$  &  $ArH(7')$ ), 8.27 (1H, d,  $ArH(8')$ ,  $J = 8.8\ Hz$ ), 8.30 (1H, d,  $ArH(2')$ ,  $J = 7.6\ Hz$ ), 8.55 (1H, d,  $ArH(4')$ ,  $J = 8.8\ Hz$ ).  $^{13}C\ NMR$  (100 MHz,  $D_2O/1,4$ -dioxane):  $\delta$  38.32, 46.43, 49.54, 51.90, 52.67, 52.89, 53.56, 56.09, 57.11, 117.58, 120.27, 125.54, 130.28, 130.42, 130.52, 131.63, 131.99, 134.72, 152.43, 175.39, 176.54. Anal. Calcd for  $C_{28}H_{52}N_{11}O_{14.5}SZn$ : C, 38.56; H, 6.01; N, 17.66. Found: C, 38.54; H, 6.01; N, 17.41.

**Crystallographic Study of  $Y^{3+}-H_{-1}L^2 \cdot 2(NO_3^-) \cdot 2.5H_2O$  (**12a**).** A colorless prismatic crystal of  $Y^{3+}-H_{-1}L^2 \cdot 2(NO_3^-) \cdot 2.5H_2O$  (**12a**) ( $C_{28}H_{49}N_{11}O_{13.5}SY$ ,  $M_r = 876.73$ ) having approximate dimensions of 0.25 mm  $\times$  0.10 mm  $\times$  0.10 mm was mounted in a loop, which was then flash-cooled in a cold gas stream (0.5  $H_2O$  was not observed in the crystal). All measurements were made on a Rigaku RAXIS-RAPID imaging plate diffractometer with graphite-monochromated Cu  $K\alpha$  radiation. Indexing was performed from three oscillations, which were exposed for 1.0 min. The camera radius was 127.40 mm. Readout was performed in the 0.100 mm pixel mode. Cell constants and an orientation matrix for data collection corresponded to a primitive monoclinic cell with dimensions  $a = 18.912(3)\ \text{\AA}$ ,  $b = 17.042(3)\ \text{\AA}$ ,  $c = 24.318(4)\ \text{\AA}$ ,  $\beta = 95.99(1)^\circ$ , and  $V = 7794(2)\ \text{\AA}^3$ . For  $Z = 8$  and  $M_r = 876.73$ , the calculated density ( $D_{calcd}$ ) was 1.49  $g\ cm^{-3}$ . On the basis of the systematic absence of  $h0l$  ( $l \neq 2n$ ) and  $0kl$  ( $k \neq 2n$ ) packing considerations, a statistical analysis of intensity distribution, and the successful solution and refinement of the structure, the space group was determined to be  $P2_1/c$  (No. 14). The data were collected at a temperature of  $-170 \pm 1\ ^\circ C$  to a maximum  $2\theta$  value of  $120.0^\circ$ . A total of 36 images, corresponding to  $900.0^\circ$  oscillation angles, were collected with nine different goniometer settings. The exposure time was 1.50 min per degree. Data were processed by using the PROCESS-AUTO program package. Of the 59 475 reflections which were collected, 13 857 were unique ( $R_{int} = 0.089$ ); equivalent reflections were merged. The linear absorption coefficient,  $\mu$ , for Cu  $K\alpha$  radiation is  $32.7\ cm^{-1}$ . A symmetry-related absorption correction using the program ABSCOR was applied which resulted in transmission factors ranging from 0.52 to 0.72. The data were corrected for Lorentz and polarization effects. The structure was solved by direct methods (SIR97) and expanded by means of Fourier techniques (DIRDIF 94). Nitrate ions were refined isotropically as rigid groups. Of the four ions, three are disordered at the two locations represented by the corresponding unprimed and primed numbers. Hydrogen atoms, excluding those of water, were included but not refined. The final cycle of full-matrix least-squares refinement was based on 10 373 observed reflections ( $I > 0.00\sigma(I)$ ,  $2\theta < 120.00$ ) and 887 variable parameters and converged (largest parameter shift was 0.00 times its esd) with unweighted and weighted agreement factors of  $R = \sum(F_o^2 - F_c^2)/\sum F_o^2 = 0.160$ .  $R_w = (\sum w(F_o^2 - F_c^2)/\sum w(F_o^2)^{0.5}) = 0.229$ . The standard deviation of an observation of unit weight was 1.48. The weighting scheme was based on counting statistics and included a factor ( $p = 0.072$ ) to downweight the intense reflections. Plots of  $\sum w(|F_o| - |F_c|)^2$  versus  $|F_o|$ , reflection order in data collection,  $\sin \theta/\lambda$ , and various classes of indices showed no unusual trends. The maximum and minimum peaks on the final difference Fourier map corresponded to 2.42 and  $-1.33\ e^{-\text{\AA}^{-3}}$ , respectively. Neutral atom scattering factors were taken from Cromer and Waber (*International Tables for X-ray Crystallography*, Vol. IV; The Kynoch Press: Birmingham, England, 1974; Table 2.2 A). All calculations were performed with the teXsan crystal structure analysis package developed by Molecular Structure Corp. (1985, 1999).

**Crystallographic Study of  $Zn^{2+}-L^2 \cdot 2(NO_3^-) \cdot 3H_2O$  (**11c**).** A yellow prismatic crystal of  $Zn^{2+}-L^2 \cdot 2(NO_3^-) \cdot 3H_2O$  (**11c**) ( $C_{28}H_{51}N_{11}O_{14}SZn$ ,  $M_r = 863.22$ ) having approximate dimensions of 0.40 mm  $\times$  0.10 mm  $\times$  0.10 mm was mounted in a loop (0.5  $H_2O$  was not observed in the crystal). All measurements were made on a Rigaku RAXIS-RAPID imaging plate diffractometer with graphite-monochromated Mo  $K\alpha$

radiation. Indexing was performed from five oscillations which were exposed for 20.0 min. The camera radius was 127.40 mm. Readout was performed in the 0.100 mm pixel mode. Cell constants and an orientation matrix for data collection corresponded to a C-centered monoclinic cell with dimensions  $a = 35.361(1) \text{ \AA}$ ,  $b = 13.7298(5) \text{ \AA}$ ,  $c = 18.5998(6) \text{ \AA}$ ,  $\beta = 119.073(2)^\circ$ , and  $V = 7892.3(5) \text{ \AA}^3$ . For  $Z = 8$  and  $M_r = 863.22$ , the calculated density ( $D_{\text{calcd}}$ ) was  $1.45 \text{ g}\cdot\text{cm}^{-3}$ . On the basis of the systematic absence of  $hkl$  ( $h + k \neq 2n$ ) and  $h0l$  ( $l \neq 2n$ ) packing considerations, a statistical analysis of intensity distribution, and the successful solution and refinement of the structure, the space group was determined to be  $C2/c$  (No. 15). The data were collected at a temperature of  $-150 \pm 1 \text{ }^\circ\text{C}$  to a maximum  $2\theta$  value of  $50.0^\circ$ . A total of 55 images, corresponding to  $220.0^\circ$  oscillation angles, were collected with two different goniometer settings. The exposure time was 5.00 min per degree. Data were processed by using the PROCESS-AUTO program package. Of the 33 737 reflections which were collected, 6959 were unique ( $R_{\text{int}} = 0.076$ ); equivalent reflections were merged. The linear absorption coefficient,  $\mu$ , for Mo  $K\alpha$  radiation is  $7.5 \text{ cm}^{-1}$ . A symmetry-related absorption correction using the program ABCOR was applied which resulted in transmission factors ranging from 0.65 to 0.93. The data were corrected for Lorentz and polarization effects. The structure was solved by direct methods (SHELXS86) and expanded by means of Fourier techniques (DIRDIF 94). Some non-hydrogen atoms were refined anisotropically, while the rest were refined isotropically. Hydrogen atoms were included but not refined. The final cycle of full-matrix least-squares refinement was based on 6125 observed reflections ( $I > 0.00\sigma(I)$ ,  $2\theta < 50.00$ ) and 438 variable parameters and converged (largest parameter shift was 0.00 times its esd) with unweighted and weighted agreement factors of  $R = \sum(F_o^2 - F_c^2)/\sum F_o^2 = 0.155$ .  $R_w = (\sum w(F_o^2 - F_c^2)^2 / \sum w(F_o^2)^2)^{0.5}$ . The standard deviation of an observation of unit weight was 1.09. The weighting scheme was based on counting statistics and included a factor ( $p = 0.011$ ) to downweight the intense reflections. Plots of  $\sum w(|F_o| - |F_c|)^2$  versus  $|F_o|$ , reflection order in data collection,  $\sin \theta/\lambda$ , and various classes of indices showed no unusual trends. The maximum and minimum peaks on the final difference Fourier map corresponded to 2.60 and  $-1.36 \text{ e}^- \cdot \text{\AA}^{-3}$ , respectively. Neutral atom scattering factors were taken from Cromer and Waber (*International Tables for X-ray Crystallography*, Vol. IV; The Kynoch Press: Birmingham, England, 1974; Table 2.2 A). All calculations were performed using the teXsan crystal structure analysis package developed by Molecular Structure Corp. (1985, 1999).

**Potentiometric pH Titrations.** The preparation of the test solutions and the calibration method of the electrode system (Orion Research Expandable Ion Analyzer EA920 and Orion Research Ross Combination

pH Electrode 8102BN) were described earlier.<sup>10,11,15</sup> All the test solutions (50 mL) were kept under an argon (>99.999% purity) atmosphere. The potentiometric pH titrations were carried out with  $I = 0.10$  (NaNO<sub>3</sub>) at  $25.0 \pm 0.1 \text{ }^\circ\text{C}$ , and at least two independent titrations were performed. Deprotonation constants and intrinsic complexation constants defined in the text were determined by means of the program BEST.<sup>16</sup> All the  $\sigma$  fit values defined in the program are smaller than 0.05. The  $K_w$  ( $=a_{\text{H}^+}a_{\text{OH}^-}$ ),  $K'_w$  ( $=[\text{H}^+][\text{OH}^-]$ ), and  $f_{\text{H}^+}$  values used at  $25 \text{ }^\circ\text{C}$  are  $10^{-14.00}$ ,  $10^{-13.79}$ , and 0.825. The corresponding mixed constants,  $K_2$  ( $=[\text{HO}^- \text{-bound species}]a_{\text{H}^+}/[\text{H}_2\text{O-bound species}]$ ), are derived using  $[\text{H}^+] = a_{\text{H}^+}/f_{\text{H}^+}$ . The species distribution values (%) against pH ( $= -\log[\text{H}^+] + 0.084$ ) were obtained using the program SPE.<sup>16</sup>

**UV Titrations and Fluorescence Titrations.** UV spectra and fluorescence emission spectra were recorded on a Hitachi U-3500 spectrophotometer and a Hitachi F-4500 fluorescence spectrophotometer, respectively, at  $25.0 \pm 0.1 \text{ }^\circ\text{C}$ . For fluorescence titrations, a sample solution in a 10 mm quartz cuvette was excited at the isosbestic point, which was determined by UV titrations. The obtained data from UV titrations (increases in  $\epsilon_{267}$  values at a given wavelength) and fluorescence titrations (increases in fluorescence emission intensity at a given wavelength) were analyzed for apparent complexation constants,  $K_{\text{app}}$ , using the program Bind Works (Calorimetry Sciences Corp). Quantum yields were determined by comparison of the integrated corrected emission spectrum of a standard quinine. Excitation at 335 nm was used for quinine in 0.10 M H<sub>2</sub>SO<sub>4</sub>, whose quantum yield was 0.54.<sup>11a</sup>

**Acknowledgment.** E.K. is thankful for the Grant-in-Aid for Priority Project "Biometallics" (No. 08249103) from the Ministry of Education, Science and Culture in Japan. S.A. is thankful for the Grant-in-Aid for Young Scientists (No. 10771249 and 12771355) and the grants from Nissan Science Foundation and Uehara Memorial Foundation. T.G. is thankful for the Graduate Scholarship from the Japan Society for the Promotion of Science. We are grateful for being allowed the use of NMR instruments (JEOL Alpha (400 MHz)) in the Research Center for Molecular Medicine (RCMM), Hiroshima University.

**Supporting Information Available:** <sup>1</sup>H NMR spectra (dansyl region) of **4**, **11c**, **12a**, and **12b**, and CIF data for **11c** and **12a**. This material is available free of charge via the Internet at <http://pubs.acs.org>.

JA0033786